Applied Optics

Huijuan Dong
Harbin Institute of Technology

Dependence of Brillouin frequency shift on radial and axial strain in silica optical fibers

Haidong Gu,[1] Huijuan Dong,[2,*] Guangyu Zhang,[1] Yongkang Dong,[3] and Jun He[1]

[1]School of Mechatronics Engineering, Harbin Institute of Technology, Harbin 150001, China

[2]State Key Laboratory of Robotics and Systems, Harbin Institute of Technology, Harbin 150001, China

[3]Institute of Opto-Electronics, Harbin Institute of Technology, Harbin 150001, China

*Corresponding author: dhj@hit.edu.cn

Received 7 August 2012; revised 18 October 2012; accepted 19 October 2012;
posted 19 October 2012 (Doc. ID 173933); published 9 November 2012

Brillouin frequency shift (BFS) in a single-mode optical fiber has been measured as a function of both radial and axial strain via the Brillouin optical time domain analysis technique. The effects of the two kinds of strain on the BFS are decoupled by making fiber pretensioned and relaxed while applying pressure. Linear relations have been found between the BFS and both kinds of strain. The radial strain coefficient $C_{v\varepsilon(r)}$ is found to be 0.029 MHz/με, and the axial strain coefficient $C_{v\varepsilon(a)}$ is 0.053 MHz/με. The result may give impetus to some potential applications of the optical fibers, such as a distributed pressure sensor based on Brillouin scattering. © 2012 Optical Society of America

OCIS codes: 060.4370, 120.5820, 060.2370, 060.2400.

1. Introduction

Stimulated Brillouin scattering (SBS) in optical fibers has been employed in numerous applications [1–3]. SBS occurs when light is propagating along an optical fiber and interacts with acoustic waves. Meanwhile, a backward-scattered light is generated by the Bragg reflecting to form the Brillouin gain spectrum (BGS), which suffers a Doppler shift [2,4]. This Doppler shift is known as Brillouin frequency shift (BFS), which is proportional to the local longitudinal acoustic velocity (V_a) and the effective refractive index (n) in the fiber [5–9]:

$$v_B = 2nV_a/\lambda_P, \tag{1}$$

where v_B is the value of the BFS and λ_P is the vacuum wavelength of the incident light.

Some previous reports have evaluated the variation of the BFS and its influential factors, such as doping concentration in fibers [6,8], pulse width of incident light [9], etc. And some papers have studied the dependence of the BFS on temperature and strain along the optical fiber [6–8]. For instance, the variation of the BFS (Δv_B) is measured to be proportional to the change of strain ($\Delta\varepsilon$):

$$\Delta v_B = C_{v\varepsilon}\Delta\varepsilon, \tag{2}$$

where $C_{v\varepsilon}$ is the strain coefficient of BFS. This so-called strain in previous literature has practically represented the axial (longitudinal) strain since [5] was published. In fact, it is a hybrid effect of axial strain and radial strain on the BFS, because the axial strain will commonly be accompanied with the radial strain. Although Floch and Cambon [10] experimented on the relation of the BFS and pressure, they did not analyze or explain further how the pressure-induced radial and axial strain changes the BFS. To our knowledge, there has been no experiment or discussion on the quantitative relations between the BFS and both values of radial and axial strain in silica optical fibers.

Accordingly, the main aim of this paper is to try to quantify separately the effect of the radial strain

1559-128X/12/327864-05$15.00/0

from that of the axial strain on the BFS. Thus, in Section 2 of the paper, an experiment has been carried out to measure the BFS versus pressure under conditions of the fiber pretensioned and relaxed. A steel frame has been designed to keep the fiber in different pretensioned states. Section 3 presents experimental results, which show linear relations between the BFS and pressure with different slopes for the pretensioned and the relaxed conditions. On the other hand, Section 4 calculates the pressure-induced radial and axial strain in the fiber core based on the well established pressure–strain model. Linear relations between pressure and both kinds of strain are solved for the two kinds of test conditions (pretensioned and relaxed, respectively). According to the results of experiment (Section 3) and calculation (Section 4), Section 5 deduces the relations between the BFS and both values of radial and axial strain by solving simultaneously the two kinds of conditions. It is found that the BFS is dependent linearly on both the radial and axial strain. In addition, a theoretical expression of this relationship has been established with the radial strain coefficient and the axial strain coefficient of the BFS. Finally, in Section 6, discussion and inference will be made by associating the result with corresponding data of previous reports.

2. Experimental Procedure

The following experiment was done with a single-mode silica optical fiber by the Brillouin optical time domain analysis (BOTDA) technique [8–11], which is a well developed method for measuring the BFS along the fiber. The block diagram of the main components is illustrated in Fig. 1.

The output of a high-frequency resolution laser (distributed feedback laser diode) at 1552.3 nm wavelength was divided by a coupler into two parts,

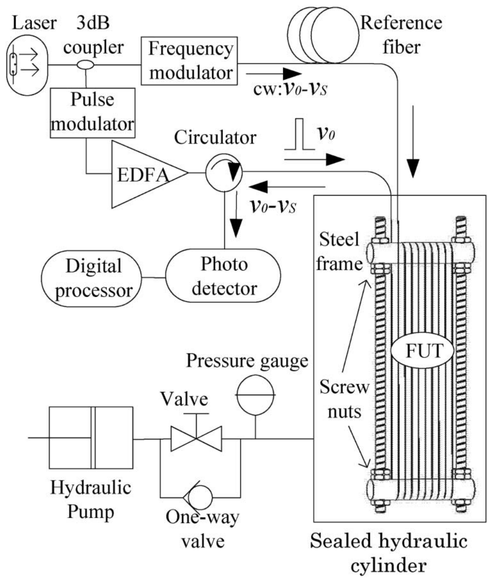

Fig. 1. Experimental arrangement for detecting BFS in the FUT with changeable radial and axial strain.

which are called pump wave and probe wave. The pump wave at frequency v_0 was preset to have a 50 ns pulse width and 45 μs repeat period. The probe wave was a continuous wave of Stokes frequency. Its frequency was downshifted by v_s from v_0, where v_0 was constant while v_s stepped over the frequency range 10.5–11.5 GHz with an interval of 2 MHz. The two waves were counterpropagating through the fiber core in opposite directions. When they met each other at a certain point in the fiber and their frequency difference was close to the BFS (i.e., $v_s = v_B$, to be precise), the probe wave would receive gain. The gain signal as a function of position along the fiber was detected by a photodetector and sent to a digital processing system. The average time was 1000, that is, the gain signal at any frequency was averaged from 1000 times measured values for any test point along the fiber. So, the BFS could be scanned by sweeping v_s and the gain signals.

This room-temperature (constant temperature at 21°C) experiment was performed on a 70 m long standard telecommunication single-mode fiber (G652.D from Yangtze Optical Fibre and Cable Company Ltd., China). The structure of this fiber under test (FUT) is shown in Fig. 2. It had a thin acrylate polymer coating. The effective group index of refraction n is 1.467 at ~1550 nm, and this 70 m long fiber as the FUT was wound and fixed around the steel frame in an orderly and uniform way to keep the fiber vertical and parallel. The frame could stretch by both sides of the screw rods and nuts (as shown in Fig. 1), so that the FUT could be pretensioned by the adjustable frame and thus the axial strain of the FUT could be controlled by the two pairs of screw nuts on the steel frame.

In order to induce radial strain on the FUT, a hydraulic system was constructed to apply pressure on the FUT. The pressure was produced by a hydraulic pump, and hydraulic oil was pumped to a sealed hydraulic cylinder, which contained the FUT. A commercial pressure gauge measured the pressure. The fiber passed through two holes on the cylinder cover, and both holes were sealed by epoxy adhesive.

The FUT was pressurized under two kinds (four sets) of test conditions, which were pretensioned (2000, 3000, and 4000 με) and relaxed (without pretension). Pressure was increased gradually up to 30 MPa with 6 MPa steps at intervals of 15 min for each set of pretension. To avoid coincidence or accident, 50 different measuring points were chosen from the FUT to be averaged in every cycle of pressurizing. A 300 m long immobile reference fiber was used to demonstrate that temperature remained stable and the optical detecting system worked

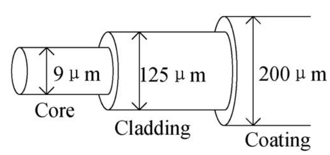

Fig. 2. Structure of the FUT.

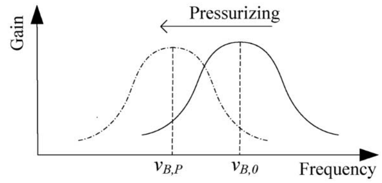

Fig. 3. Overview of the variation of BGS as pressurizing (solid curve, BGS without pressure; dotted curve, BGS under pressure).

properly as long as the BFS of the reference fiber normally remained constant during the test procedure.

3. Measured Relations between BFS and Pressure

Figure 3 presents an overview of the variation of the BGS as pressurizing for a certain test point along the FUT. It shows clearly that the BFS under pressure ($v_{B,P}$) is smaller than the BFS without pressure ($v_{B,0}$). Figure 4 plots the 50 points' average values of the BFS (v_B) against pressure (P) under different sets of test conditions. It indicates that v_B decreases linearly and negatively with P, and the slopes are −0.418, −0.413, −0.404, and −0.752 MHz/MPa for a pretension of 2000, 3000, and 4000 με and relaxed, respectively. It is obvious that the slopes are almost equal among the three sets of pretension conditions. −0.412 MHz/MPa, as the average value of the three slopes, is taken for the following calculation, so when the FUT is relaxed before pressurizing,

$$\Delta v_B = -0.752(\mathrm{MHz}\cdot\mathrm{MPa}^{-1})\cdot\Delta p, \qquad (3)$$

and when the FUT is pretensioned before pressurizing,

$$\Delta v_B = -0.412(\mathrm{MHz}\cdot\mathrm{MPa}^{-1})\cdot\Delta p. \qquad (4)$$

4. Calculated Relations between Pressure and Strain

The FUT is composed of core, cladding, and coating, as shown in Fig. 2. Thus the FUT's strain due to pressure must be calculated by considering its geometry and mechanical properties. For a long slender cylindrical fiber with m layers, the relation between pressure and strain in radial, tangential, and axial dimensions of the fiber can be established as the pressure–strain model (Eqs. (2)–(9) in [12]) by the

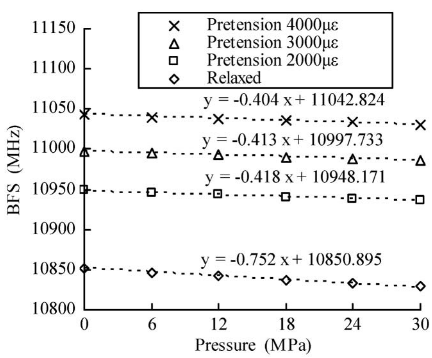

Fig. 4. Pressure dependence of the BFS in the FUT under different sets of test conditions.

combination of Lame solutions and boundary conditions. As is known, core and cladding have similar mechanical properties to silica glass, so they are considered as one layer (the layer zero), i.e., there are two layers in this analysis. The only difference between the two kinds of test conditions (the pretensioned and the relaxed) in that pressure–strain model is the right term of Eq. (8) in [12]: an extra force determined by pretension must be added to the right term of that Eq. (8) for the conditions of pretensioned.

Given by the supplier, the estimated values of the two layers' parameters (radius, Poisson's ratio, and Young's modulus, respectively) are $r_0 = 62.5$ μm, $r_1 = 100$ μm, $\lambda_0 = 0.17$, $\lambda_1 = 0.4995$, $E_0 = 72$ GPa, $E_1 = 0.007$ GPa. The variations of axial and radial strain in the core of the FUT [$\Delta\varepsilon(a)_0$, $\Delta\varepsilon(r)_0$] can be evaluated by that pressure–strain model for both kinds of test conditions.

Specifically, when the FUT is relaxed before pressurizing,

$$\Delta\varepsilon(a)_0 = -9.18\times10^{-6}(\mathrm{MPa}^{-1})\cdot\Delta P, \qquad (5)$$

$$\Delta\varepsilon(r)_0 = -9.15\times10^{-6}(\mathrm{MPa}^{-1})\cdot\Delta P. \qquad (6)$$

When the FUT is pretensioned before pressurizing, $\Delta\varepsilon(a)_0$ is restricted to follow with the axial strain of the steel frame while pressurizing. Thus, $\Delta\varepsilon(a)_0$ can be calculated by

$$\Delta\varepsilon(a)_0 = \Delta\varepsilon(a)_f = -\Delta P(1-2v_f)/E_f, \qquad (7)$$

where $\Delta\varepsilon(a)_f$ is the change of the frame's axial strain induced by pressure. E_f and v_f are Young's modulus and Poisson's ratio of the frame, respectively. For this steel frame, $E_f = 210$ GPa, $v_f = 0.28$. By substituting the values of E_f and v_f into Eq. (7),

$$\Delta\varepsilon(a)_0 = -2.10\times10^{-6}(\mathrm{MPa}^{-1})\cdot\Delta P. \qquad (8)$$

Then $\Delta\varepsilon(r)_0$ can be solved from the pressure–strain model:

$$\Delta\varepsilon(r)_0 = -10.36\times10^{-6}(\mathrm{MPa}^{-1})\cdot\Delta P. \qquad (9)$$

Therefore, two pairs of equations [Eqs. (5) and (6), (8) and (9)] have been acquired to describe the increment in both radial and axial strain per unit pressure for the two test conditions.

5. Deduced Relations of BFS and Strain

Experimental results above have shown the linear relations between the BFS and pressure. And it has also been confirmed from the calculation that both radial and axial strain in the fiber core have linear relations with pressure as well. Therefore, it can be assumed that the BFS has a linear dependence upon both radial and axial strain. Supposing that the temperature remains constant, Δv_B can be expressed by a linear combination of $\Delta\varepsilon(a)_0$ and $\Delta\varepsilon(r)_0$:

$$\Delta v_B = c_{v\varepsilon(r)}\Delta\varepsilon(r)_0 + c_{v\varepsilon(a)}\Delta\varepsilon(a)_0, \tag{10}$$

where $C_{v\varepsilon(r)}$ and $C_{v\varepsilon(a)}$ are the radial and axial strain coefficients of the BFS, respectively. By substituting Eqs. (3), (5), and (6) into Eq. (10) and substituting Eqs. (4), (8), and (9) into Eq. (10), $C_{v\varepsilon(r)}$ and $C_{v\varepsilon(a)}$ can be deduced to be 0.029 and 0.053 MHz/με.

To the best of our knowledge, this is the first instance of experimenting and evaluating the dependence of the BFS on the radial strain and the axial strain, respectively, within the silica optical fiber.

6. Discussion

For the relaxed condition, the experimental slope (−0.752 MHz/MPa) of the BFS versus pressure is less than previous experimental value (−0.92 MHz/MPa) in [10]. This difference may come from different coatings, as the same pressure can induce different strains in the fiber core due to different coatings. However, there is no mention in [10] of the influence of the coating nor analysis of the two kinds of strain induced by pressure.

The experimental slopes seem to decrease slightly at higher pretension for the three sets of pretensioned conditions. This decrease probably results from the general error in the experimental system, or even from the potential fact that the BFS would be less sensitive to pressure at higher pretension. Nevertheless, that slight decrease is neglected, as the differences among those three slope values are trivial (less than 5% of the difference between the pretensioned and relaxed conditions). That is to say, the pretensioned value does not obviously influence the slope of the BFS versus pressure.

In fact, when lateral pressure or radial stress on the fiber core is slight or negligible, $\Delta\varepsilon(r)_0$ is proportional to $\Delta\varepsilon(a)_0$ by Poisson's ratio of the core (λ_c), that is,

$$\Delta\varepsilon(r)_0 = -\lambda_c\Delta\varepsilon(a)_0. \tag{11}$$

Substituting Eq. (11) into Eq. (10), we can obtain the same form as Eq. (2):

$$\Delta v_B = [C_{v\varepsilon(a)} - \lambda_c C_{v\varepsilon(r)}]\Delta\varepsilon(a)_0. \tag{12}$$

Correspondingly, $[C_{v\varepsilon(a)} - \lambda_c C_{v\varepsilon(r)}]$ shall be the same as $C_{v\varepsilon}$ in Eq. (2). Commonly, when $\lambda_c = 0.17$, $[C_{v\varepsilon(a)} - \lambda_c C_{v\varepsilon(r)}]$ can be calculated, from our results above, to be 0.0481 MHz/με. It is consistent with the previous experimental value in [7], in which $C_{v\varepsilon}$ is 0.0483 MHz/με What's more, when pressure was zero in our experiment, v_B was measured to be 10851.2, 10948.2, 10995.8, and 11043.5 MHz for the conditions of relaxed and with a pretension of 2000, 3000, and 4000 με, respectively, as shown in Fig. 4. These values are in good agreement with Eq. (12). So, $C_{v\varepsilon}$ in Eq. (2) is actually the combination coefficient of $C_{v\varepsilon(r)}$ and $C_{v\varepsilon(a)}$ in Eq. (10). And this paper has originally experimented with dividing $C_{v\varepsilon}$ into $C_{v\varepsilon(r)}$ and $C_{v\varepsilon(a)}$, which are essential in obtaining the BFS in the fibers from the radial and axial strain, especially when the radial strain is no longer commonly proportional to the axial strain. For example, fiber suffers hydrostatic pressure.

This experiment can be complementary to the experiment in [5]. Yet it should be noted that both kinds of strain represent the strain in the fiber core, not the coating or jacket. Since same pressure can induce varying strain in the fiber core due to different coatings, the result of this experiment can be employed in designing distributed pressure sensing in downhole.

According to Eq. (10), the BFS can be changed by the radial strain as well as the axial strain. And from Eq. (1), both the acoustic velocity and the effective refractive index in the fiber can also be influenced by the radial and axial strain. Moreover, the effect of the axial strain on the BFS is more obvious than that of the radial strain. It can probably be inferred that the distance between atoms in the axial dimension (along the optical light path) affects the BFS rather more than that in the radial dimension (in the plane vertical to the light path). This inference is interesting, and its physical meaning will be very complex and hard to confirm immediately. Our future work will focus on it.

7. Conclusion

This paper has been concerned with the dependence of the BFS on both radial and axial strain in silica optical fibers.

A steel frame was designed to keep the fiber under two test conditions (the pretensioned and the relaxed) while applying hydrostatic pressure so that the radial and axial strain could be decoupled. By combining the two test conditions, the effects of radial and axial strain on the BFS can be distinguished. The results show excellent linear relations between the BFS and both radial and axial strain in the fiber core. For the fiber used in our experiment, its coefficients $C_{v\varepsilon(r)}$ and $C_{v\varepsilon(a)}$ are measured to be 0.029 and 0.053 MHz/με. This work can open a way to distributed pressure sensing along the fiber. It may also provide a reference for designing submarine fiber telecommunications.

The authors gratefully express their sincere thanks to L. Zou of OZ Optics Limited for helpful discussions. This research is sponsored by the National Natural Science Foundation of China under Grant No. 51074059, "Full-life health online-monitoring for oil-water well casing by distributed fiber sensing system on multi-field coupling effect."

References

1. T. Kurashima, T. Horiguchi, and M. Tateda, "Distributed-temperature sensing using stimulated Brillouin scattering in optical silica fibers," Opt. Lett. **15**, 1038–1040 (1990).
2. A. Kobyakov, M. Sauer, and D. Chowdhury, "Stimulated Brillouin scattering in optical fibers," Adv. Opt. Photon. **2**, 1–59 (2010).
3. X. Bao and L. Chen, "Recent progress in Brillouin scattering based fiber sensors," Sensors **11**, 4152–4187 (2011).

4. K. Brown, A. W. Brown, and B. G. Colpitts, "Characterization of optical fibers for optimization of a Brillouin scattering based fiber optic sensor," Opt. Fiber Technol. **11**, 131–145 (2005).
5. T. Horiguchi, T. Kurashima, and M. Tateda, "Tensile strain dependence of Brillouin frequency shift in silica optical fibers," IEEE Photonics Technol. Lett. **1**, 107–108 (1989).
6. M. Nikles, L. Thevenaz, and P. A. Robert, "Brillouin gain spectrum characterization in single-mode optical fibers," J. Lightwave Technol. **15**, 1842–1851 (1997).
7. T. R. Parker, M. Farhadiroushan, V. A. Handerek, and A. J. Rogers, "Temperature and strain dependence of the power level and frequency of spontaneous Brillouin scattering in optical fibers," Opt. Lett. **22**, 787–789 (1997).
8. W. Zou, Z. He, and K. Hotate, "Investigation of strain- and temperature-dependences of Brillouin frequency shifts in GeO_2-doped optical fibers," J. Lightwave Technol. **26**, 1854–1861 (2008).
9. S. B. Cho, Y. G. Kim, J. S. Heo, and J. J. Lee, "Pulse width dependence of Brillouin frequency in single mode optical fibers," Opt. Express **13**, 9472–9479 (2005).
10. S. L. Floch and P. Cambon, "Study of Brillouin gain spectrum in standard single-mode optical fiber at low temperatures (1.4–370 K) and high hydrostatic pressures (1–250 bars)," Opt. Commun. **219**, 395–410 (2003).
11. Y. Dong, L. Chen, and X. Bao, "Extending the sensing range of Brillouin optical time-domain analysis combining frequency-division multiplexing and in-line EDFAs," J. Lightwave Technol. **30**, 1161–1167 (2012).
12. N. Lagakos and J. A. Bucaro, "Pressure desensitization of optical fibers," Appl. Opt. **20**, 2716–2720 (1981).